Non-Fourier heat transfer enhancement in Power law fluid with mono and hybrid nanoparticles

M. Adil Sadiq (adilsadiq@kfupm.edu.sa)
DCC-KFUPM

Research Article

Keywords: Non-Fourier heat transfer, hybridity of nanoparticles, numerical heat transfer, thermal relaxation, heat generating uid

Posted Date: May 18th, 2021

DOI: https://doi.org/10.21203/rs.3.rs-532422/v1

Non-Fourier heat transfer enhancement in Power law fluid with mono and hybrid nanoparticles

M. Adil Sadiq[a,1]

[a]Department of Mathematics, DCC-KFUPM, Box 5084, Dhahran, 31261, Saudi Arabia

Abstract: Several polymers like ethylene glycol exhibit non-Newtonian rheological behaviors. Ethylene glycol is a world-widely used engine coolant and therefore, investigation of thermal enhancement by dispersing mono and hybrid nanoparticles in ethylene glycol is worthful. Since, ethylene glycol has shear rate-dependent viscosity and it obeys the power law rheological model. Therefore, based on these facts, the power-law rheological model is used with thermophysical properties are augmented with basic laws of heat transfer in fluid for the modeling of considered physical situations. MoS_2 are taken as mono- nanoparticles where MoS_2 and SiO_2 are taken as hybrid nano-sized particles. Comparative study for the enhancement of thermal performance of MoS_2 ethylene glycol and MoS_2-SiO_2- ethylene glycol is done. For energy conservation, non-Fourier's law of Cattaneo- Christov is used. Power law fluid becomes more heat generative due to dispersion of MoS_2 and SiO_2. However, MoS_2-power law fluid is less heat generative relative to $MoS_2 - SiO_2$-nanofluid. Thermal relaxation time is found proportional to the ability of the fluid to restore its thermal equilibrium.

Keywords: Non-Fourier heat transfer; hybridity of nanoparticles; numerical heat transfer; thermal relaxation; heat generating fluid

1 Introduction

Natural and industrial fluids show deviation from Newton's law of viscosity because their viscosity does not show linear relation with the rate of deformation. Such fluids are called non-Newtonian fluids. Non-Newtonian fluids are further classified into many classes. Shear rate-dependent non-Newtonian fluids is a well-known class of non-Newtonian fluid. Shear rate-dependent viscosity fluids are further classified into power-law fluid [1], Carreau fluids [2], Carreau-Yasuda fluid [3], Bingham fluids [4], Casson fluids [5], Herschel–Bulkley [6], etc. Power-law fluid model is used here in this study. Power law model is chosen as it best describes the rheological behavior of ethylene glycol [7]. In this study, the thermal

[1]Corresponding author : +966 598658229

email: adilsadiq@kfupm.edu.sa

performance of ethylene glycol is aimed to be discussed. The reason for the selection of power law model for rheology of ethylene glycol is because of recent work by [7]. Although this rheological model has been used in several studies but here, we discuss only those which related to the present investigation. For example, Nawaz et al. [8] discussed two-dimensional heat transfer enhancement in power law fluid by considering hybrid nanofluid. Cheng [9]discussed simultaneous transport of heat and mass in power law fluid subjected to mass and thermal stratification over a vertical wavy surface. Khan et al. [10] performed theoretical analysis for heat and mass transfer in power law fluid over a surface subjected to convective boundary conditions. Sarafan et al. [11] examined heat and mass transfer in power law fluid in a microchannel immersed in a pourous medium. Pal and Chatterjee [12] analyzed Soret and Dufour effects on heat and mass transfer in power fluid over a vertical surface subjected to Buoyancy force considering variable thermal conductivity. El-Kabeir et al. [13] discussed the impact of stagnation point flow on heat and mass transfer in power law fluid over moveable walls with the consideration of combined effects of Soret and Dufour and chemical reaction.

Heat transfer has its importance as it occurs in many natural and man-made processes. Heat exchangers, thermal and cooling systems, applications related to heat and mass transfer, energy storage, solar systems related applications, MHD generators, food processing processes, etc. are well-known processes where heat transfer is an integral part. The studies related to heat transfer are numerous. However, here, we describe the investigations which are mostly related to present work. For examples, [14-20].

The efficiency of the process related to heat transfer can be enhanced by using working fluids with higher thermal conductivity. The thermal conductivity of working fluid by dispersion of nanoparticles in it can be enhanced. This dispersion of nanoparticles is possible now as synthesis and dispersion of such nanoparticles in a base fluid is possible due to the advancement in technology. Having this fact in mind, researchers have analyzed the role of nanoparticles on thermal enhancement. For example, Nawaz et al.[21] discussed the role of suspension of nanoparticles on an enhancement in partially ionized fluid during mass transport of species. Qureshi et al.[22] studied the role of suspension of nanoparticles on heat transfer in magnetohydrodynamic flow exposed to the magnetic field of constant intensity in the presence of mass transfer and chemical reaction. Ellahi et al. [23] examined the role of nanoparticles on heat transfer in blood moving under the peristaltic mechanism in a couple

of stress fluids. Sheikholeslami et al. [24] visualized the impact of dispersion of nanoparticles on heat transfer in MHD fluid moving in a porous medium. Sandeep and Kumar [25] considered suspension of nanoparticles in fluid flow subjected to simultaneous transport of heat and mass. Qi et al. [26] modeled heat transfer in the fluid under the influence of suspension of nanoparticles and relaxed the problems using the Lattice Boltzmann approach to visualize thermal enhancement in the fluid. Gheynani et al. [27] examined the effect of the size of nanoparticles on heat transfer in non- Newtonian fluid flow. They considered carboxymethyl cellulose as a base fluid.

As far as thermal enhancement of heat transfer is concerned, the dispersion of hybrid nanoparticles (nanoparticles of more than one kind) is recommended as this dispersion of hybrid nanoparticles results an optimized enhancement of heat transfer. The recent works on hybrid nanofluids can be mentioned through references. Ahmad et al. [28] discussed the impact of simultaneous dispersion of copper and aluminum oxide on heat transfer and mass transport in the fluid passing through a porous medium. Ghadikol et al. [29] considered the dispersion of TiO_2 and CuO in the mixture of ethylene glycol and water and analyzed their impact on heat transfer enhancement. Alharbi [30] and Ramesh et al. 31] performed numerical simulations related to the enhancement of heat transfer in the fluid. Hossein et al. [32] noted the optimized heat transfer in fluid containing hybrid nanoparticles. Sreedevi et al. [33] and Alharbi et al. [34] recommended the dispersion of hybrid nanoparticles for optimized enhancement in thermal transport in the fluid.

It has been proved that fluids with shear rate-dependent viscosity can restore their thermal equilibrium state due to thermal relaxation time characteristics. To analyze such characteristics, classical Fourier's law of heat conduction can not be used in the formulation of energy transfer in fluids as this law does not involve thermal relaxation time. Due to this fact, Cattaneo [35] and Christov [36] proposed the modified form of Fourier's law of heat conduction. After Cattaneo- Christov theory, several researchers have used this theory in their investigations. Siu et al. [37] used Cattaneo-Christove heat flux theory for the formulation of problems for double diffusion in Maxwell fluid. They examined the impact of thermal relaxation time on heat transfer in the fluid. Hafeez et al. [38] developed models for transfer of heat in Oldroyd-B fluid using non-Fourier's law of Cattaneo-Christove and they examined the role of momentum relaxation time and thermal relaxation time on momentum diffusion and heat transfer respectively. Makinde et al. [39] published on numerical heat

transfer in MHD fluid flow by applying Cattaneo- Chritov heat flux model. Bai et al. [40] analyzed the combined effects of stagnation point flow and thermal relaxation time on heat transfer in Oldroyd-B fluid. Similar studies related Cattaneo- Christov can be seen in refs [41, 42].

Authors through literature survey, knew that no study on three-dimensional heat transfer enhancement in power law fluid (ethylene glycol) due to the simultaneous dispersion of MoS_2 and SiO_2 has been investigated yet. The physical model and geometry of the problem is described in Figure 1. Further, such problems for heat transfer enhancement as modeled in this case have not been solved by the finite element method (FEM). This investigation covers these two aspects mentioned above. This investigation consists of five sections. Section one is the background of this problem. Models and their formulation is given in section two. The numerical method is discussed in section three. Outcomes are described in section four. The key outcomes are listed in section five.

2 Modeling and models

Power law rheological models are capable of exhibiting shear rate-dependent viscosity. Several industrial products during the thermal process behave as shear rate-dependent fluid. Modern research has revealed that fluid with shear rate-dependent viscosity, does not obey the classical law of heat conduction. Therefore, we model transfer in the power law fluid using non-classical law of heat conduction. This is the non-Fourier law of heat conduction was proposed by Cattaneo [35] and Christov [36]. Thus governing laws and power law constitutive models are simultaneously used for the development of the problem.

Let us consider two-dimensionally moving stretchable surface having constant temperature T_w. The surface is moving with velocity $\mathbf{V}_w = ax\hat{\imath} + by\hat{\jmath}$ where a and b are constants having unit s^{-1}. Fluid over a surface is non- Newtonian and obeys the power law rheological model describing shear rate-dependent viscosity. The heat transfer process is assumed to be enhanced using nanoparticles of one kind (MoS_2) and hybrid nanoparticles (combination of MoS_2 and SiO_2). It is aimed to compare the enhancement in heat transfer in MoS_2- power law fluid and $MoS_2 - SiO_2-$ power law fluid. Comparative analysis among both types of mixtures (MoS_2- power law fluid and $MoS_2 - SiO_2-$ power law fluid) will be done based on graphical and numerical outcomes. As the wall is moving with two-dimensional velocity,

therefore the flow of fluid and heat transfer will be three-dimensional. The conservation laws will be approximated by the boundary layer approximations. Hence, approximated 3D equations are given by [43]

$$\frac{\partial u}{\partial x}+\frac{\partial v}{\partial y}+\frac{\partial w}{\partial z}=0, \tag{1}$$

$$u\frac{\partial u}{\partial x}+v\frac{\partial u}{\partial y}+w\frac{\partial u}{\partial y}=\frac{k_1}{\rho_{hnf}}\frac{\partial}{\partial z}\left(\left|\frac{\partial u}{\partial z}\right|^{n-1}\frac{\partial u}{\partial z}\right)-\frac{(B_0)^2\sigma_{hnf}}{\rho_{hnf}}(u-v), \tag{2}$$

$$u\frac{\partial v}{\partial x}+v\frac{\partial v}{\partial y}+w\frac{\partial v}{\partial y}=\frac{k_1}{\rho_{hnf}}\frac{\partial}{\partial z}\left(\left|\frac{\partial u}{\partial z}\right|^{n-1}\frac{\partial v}{\partial z}\right)-\frac{(B_0)^2\sigma_{hnf}}{\rho_{hnf}}(v+u), \tag{3}$$

$$\begin{aligned}u\frac{\partial T}{\partial x}+v\frac{\partial T}{\partial y}+w\frac{\partial T}{\partial z}+\ &\lambda_1(u^2\frac{\partial^2 T}{\partial x^2}+v^2\frac{\partial^2 T}{\partial y^2}+w^2\frac{\partial^2 T}{\partial z^2}+2uv\frac{\partial^2 T}{\partial x\partial y}+2vw\frac{\partial^2 T}{\partial y\partial z}\\ &+2uw\frac{\partial^2 T}{\partial x\partial z}+\left(u\frac{\partial u}{\partial x}+v\frac{\partial u}{\partial y}+w\frac{\partial u}{\partial z}\right)\frac{\partial T}{\partial x}-\frac{Q_0}{(\rho C_p)_{hnf}}(u\frac{\partial T}{\partial x}+v\frac{\partial T}{\partial y}+w\frac{\partial T}{\partial z})\\ &+\left(u\frac{\partial v}{\partial x}+v\frac{\partial v}{\partial y}+w\frac{\partial v}{\partial z}\right)\frac{\partial T}{\partial y}++\left(u\frac{\partial w}{\partial x}+v\frac{\partial w}{\partial y}+w\frac{\partial w}{\partial z}\right)\frac{\partial T}{\partial z})\\ &=\frac{k_{_{hnf}}}{(\rho C_p)_{_{hnf}}}\frac{\partial^2 T}{\partial^2 y}+\frac{Q_0}{(\rho C_p)_{_{hnf}}}(T-T_\infty).\end{aligned} \tag{4}$$

After implementation of noslip mechanism one can get the boundary conditions which are written below

$$\left.\begin{aligned}u=ax=U_w,\ v=by=V_w,\ T=T_w,\ w=0 \text{ at } z=0,\\ v\to 0,\ u\to 0,\ T\to T_\infty \text{ at } z\to\infty,\end{aligned}\right\}, \tag{5}$$

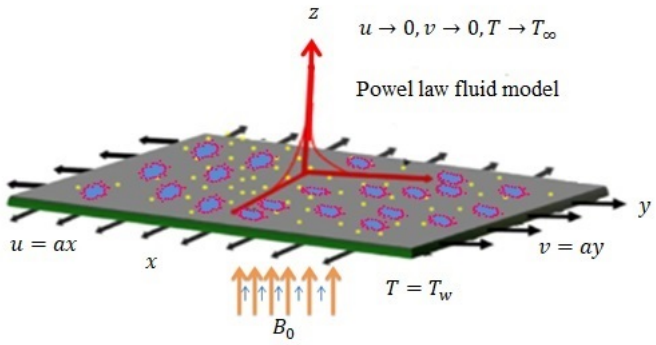

Figure 1: Physical model with coordinate representation

The velocity and temperature variables via symmetry analysis are expressed as

$$\left.\begin{aligned}u=axf',\ v=byg',\ w=-a\left(\tfrac{ba^{n-2}}{\rho_f}\right)^{\frac{1}{n+1}}\left[\tfrac{2n}{n+1}f+\tfrac{1-n}{1+n}\eta f'+g\right]x^{\frac{n-1}{n+1}}\\ \theta=\tfrac{T-T_\infty}{T_w-T_\infty},\ \eta=\left(\tfrac{ba^{n-2}}{\rho_f}\right)^{\frac{1}{n+1}}zx^{\frac{1-n}{1+n}}\end{aligned}\right., \tag{6}$$

Above relations for velocity and temperature field help to transform Eqs $(1)-(4)$ in their dimensionless forms which are

$$\left.\begin{array}{c}\left(|f''|^{n-1}f''\right)'-(1-\varphi_2)\{(1-\varphi_1)+\varphi_1\frac{\rho_{s_1}}{\rho_f}\}+\varphi_2\frac{\rho_{s_2}}{\rho_f}\left[(f')^2+\left(\frac{2n}{n+1}f+g\right)f''\right]\\ -(1-\varphi_1)^{2.5}(1-\varphi_2)^{2.5}\frac{\sigma_{hnf}}{\sigma_f}M^{2(}f'-g')=0,\\ f(0)=0,\ f'(0)=1,\ f(\infty)=0,\end{array}\right\},\quad(7)$$

$$\left.\begin{array}{c}\left(|f''|^{n-1}g''\right)'-(1-\varphi_2)\{(1-\varphi_1)+\varphi_1\frac{\rho_{s_1}}{\rho_f}\}+\varphi_2\frac{\rho_{s_2}}{\rho_f}\left[(g')^2+\left(\frac{2n}{n+1}f+g\right)g''\right]\\ -(1-\varphi_1)^{2.5}(1-\varphi_2)^{2.5}\frac{\sigma_{hnf}}{\sigma_f}M^2(g'+g')=0,\\ f(0)=0,\ f'(0)=1,\ f(\infty)=0,\end{array}\right\}$$

$$\left.\begin{array}{c}\theta''+\frac{(\rho C_p)_{hnf}k_f}{(\rho C_p)_f k_{hnf}}\left[\Pr\left(\frac{2n}{n+1}\right)f\theta'+\Pr g\theta\right]-\frac{(\rho C_p)_{hnf}k_f}{(\rho C_p)_f k_{hnf}}\Pr\lambda_E[\left(\frac{2n}{n+1}f+g\right)\left(\frac{2n}{n+1}f'+g'\right)\theta'\\ \left(\frac{2n}{n+1}f+g\right)^2\theta''+h_s\Pr\left(\frac{2n}{n+1}f\theta'+g\theta'\right)]\\ +\frac{k_f}{k_{hnf}}h_s\left(\frac{2n}{n+1}\right)\Pr\theta=0,\\ \theta(0)=1,\ \theta(\infty)=0,\end{array}\right\},$$

$$(8)$$

The quanties involved above equations are expressed by

$$\rho_{nf}\left(=(1-\varphi)\rho_f+\phi\rho_S\right),\ \rho_{hnf}\left(=[(1-\varphi_2)\{(1-\varphi_1)\rho_f+\varphi_1\rho_{S_1}\}]+\varphi_2\rho_{S_2}\right),$$
$$(\rho c_p)_{nf}\left(=(1-\varphi)(\rho c_p)_f+\varphi(\rho c_p)_S\right),\ (\rho c_p)_{hnf}\left(=\begin{array}{c}[(1-\varphi_2)\{(1-\varphi_1)(\rho c_p)_f\\ +\varphi_1(\rho c_p)_{S_1}\}]+\varphi_2(\rho c_p)_{S_2}\end{array}\right)$$

$$\mu_{nf}\left(=\frac{\mu_f}{(1-\varphi)^{2.5}}\right),\ \mu_{hnf}\left(=\frac{\mu_f}{(1-\varphi_1)^{2.5}(1-\varphi_2)^{2.5}}\right),$$
$$\frac{k_{hnf}}{k_{bf}}\left(=\frac{k_{S_2}+(n-1)k_{bf}-(n-1)\varphi_2(k_{bf}-k_{S_2})}{k_{S_2}+(n-1)k_{bf}+\varphi_2(k_{bf}-k_{S_2})}\right),\ \frac{\sigma_{nf}}{\sigma_f}\left(=(1+\frac{3(\sigma-1)\varphi}{(\sigma+2)-(\sigma-1)\varphi})\right),$$
$$\frac{\sigma_{hnf}}{\sigma_{bf}}\left(=\frac{\sigma_{S_2}+2\sigma_{bf}-2\varphi_2(\sigma_{bf}-\sigma_{S_2})}{\sigma_{S_2}+2\sigma_{bf}+\varphi_2(\sigma_{bf}-\sigma_{S_2})}\right),\ \frac{\sigma_{bf}}{\sigma_f}\left(=\frac{\sigma_{S_1}+2\sigma_f-2\varphi_1(\sigma_f-\sigma_{S_1})}{\sigma_{S_1}+2\sigma_f+\varphi_1(\sigma_f-\sigma_{S_1})}\right),$$
$$\frac{k_{nf}}{k_f}\left(=\{\frac{k_S+(n-1)k_f-(n-1)\varphi(k_f-k_S)}{k_S+(n-1)k_f+\varphi(k_f-k_S)}\}\right).$$

The dimensionless parameters are $M^2=\frac{2\sigma_f B_0^2}{a\rho_f}$, $Q_h=\frac{Q}{a(C_p)_f\rho_f}$, $\lambda_E=\frac{a\lambda_1}{x}$, $Re=\frac{x^n(U_w)^{2-n}\rho_f}{k_f}$ and $\Pr=\frac{(C_p)_f\rho_f a x^2 Re^{\frac{2}{n+1}}}{k_f}$. These dimensionless parameters, respectively are called, the Hartmann number, the heat generation parameter, the thermal relaxation parameter (thermal Deborah number), the Reynolds number and the Prandtl number. The subscripts f, hnf, nf, stands for fluid, hybrid nanofluid and nanofluid respectively. s_1 and s_2 stand for solid particles MoS_2 and SiO_2 respectively.

Stresses (in dimensionless forms) in x and $y-$ directions are

$$\frac{1}{2}C_f(Re)^{\frac{1}{n+1}} = \frac{1}{(1-\varphi_1)^{2.5}(1-\varphi_2)^{2.5}}\left|f''(0)\right|^n \tag{9}$$

$$\frac{1}{2}C_g(Re)^{\frac{1}{n+1}} = \frac{1}{(1-\varphi_1)^{2.5}(1-\varphi_2)^{2.5}}\left|f''(0)\right|^{n-1} g''(0),$$

The heat transfer rate can be determined through

$$Nu = \frac{xq_w}{K_f(T_w - T_\infty)},\ q_w = -k_{hnf}\frac{\partial T}{\partial z}|_{\text{at wall}},\ (Re)^{-0.5}Nu = -\frac{k_{hnf}}{k_f}\theta'(0). \tag{10}$$

3 Numerical method

The finite element method (FEM) is the most suitable method for CFD problems. The convergence associated with FEM can be achieved easily. Further convergence rate for FEM is faster than other methods like finite volume method, finite difference method, spectral method, etc. The working principle for FEM can consist of the following important steps.

1. Derivation of integral residual statements in their weak forms.

2. The approximation of weak forms. Here, in this investigation, the weak forms are approximated using the Galerkin procedure.

3. The derivation of stiffness elements and their use in the assembly process. The nonlinear system is obtained via the assembly process.

4. The nonlinear equations are linearized and obtained linearized system is solved iteratively.

5. Computations are performed to ensure the results to be grid-independent. The grid-independent analysis is done through numerous experiments. The outcomes are listed in Table 1

Table 1: Grid independent results when $\text{Pr} = 204,\ \lambda_E = 0.01,\ h_s = 1.3,\ n = 2,\ M = 0.001,\ \varphi_1 = 0.004,\ \varphi_2 = 0.0075$.

Number of elements	$f'(\frac{\eta_\infty}{2})$	$g'(\frac{\eta_\infty}{2})$	$\theta(\frac{\eta_\infty}{2})$
30	0.5376460453	0.5376460453	0.5546070594
60	0.5176980663	0.5176980663	0.5377861295
90	0.5115628373	0.5115628373	0.5321685164
120	0.5085855867	0.5085855867	0.5293573362
150	0.5068273585	0.5068273585	0.5276701521
180	0.5056668939	0.5056668939	0.5265445047
210	0.5048435401	0.5048435401	0.5257412993
240	0.5042290630	0.5042290630	0.5251384468
270	0.5037528152	0.5037528152	0.5246705698
300	0.5033731756	0.5033731756	0.5242942273

The numerical values for density specific heats, thermal conductivities and electrical conductivities for solid particles s_1, s_2 and the base fluid are tabulated in Table 2 given below

Table 2: The numerical values for thermophysical propertise for s_1, s_2 and base fluid

Physical properties	Ethylene glycol	MoS_2	SiO_2
ρ	1113.5	2650	5060
c_p	2430	730	397.746
k	0.613	1.5	34.5
σ	4.3×10^{-5}	0.0005	1×10^{-18}

4 Results and discussion

Rheological models, models of hybrid nanoparticles and fundamental dimensionless equations are solved numerically using FEM. After, ensuring convergence, grid-independent and validation of results, numerical experiments for the behaviors of related parameters on field variables are done. The simulations are visualized and recorded in graphical and numerical data.

Velocity components and variation of parameters: The parameter n appears in the constitutive equation for fluid called power law fluid. For $n = 1$ the model equations reduce to the case of Newtonian fluid. The case $n > 1$ is called shear thicking case. The

behavior of n on x and y components of velocity is examined and observed outcomes are displayed in Figures 2 and 3. These Figures predict that both components of velocity have decreasing tendency for values of n greater than 1. However, this declination in the case of $MoS_2 - SiO_2-$power law fluid is greater than the case of MoS_2-power law fluid. Thus viscous region for the Newtonian fluid is wider than the versus region for nano-power fluid (see Figures 2 and 3). Figures 4 and 5 determine the behavior of velocity components against the variation of Hartmann number M. An increase in M is because of an increase in the intensity of the magnetic field which is responsible for an increase in the magnitude of opposing force. Consequently, the flow of fluid slows down. This decreasing tendency of motion of fluid particles is observed in both x and y directions. Thus it is concluded that the width of the viscous region is controllable via an applied magnetic field. Figures 4 and 5 also demonstrates that the Lorentz force induced due to the motion of $MoS_2 - SiO_2-$ power law fluid is weaker than the Lorentz force induced due to the motion of Mos_2-power law fluid. Alternatively, boundary layer thickness for MoS_2-power law fluid is greater than the boundary layer region of $MoS_2 - SiO_2-$power law fluid.

Temperature filed and variation of related parameters: The behaviors of parameters n, h_s and λ_e on the temperature field are visualized through numerical simulation and observed behaviors are recorded in the form of graphs given by Figures $6-8$ for both types of fluids (MoS_2-SiO_2-power law fluid and MoS_2-power law fluid). Figure 6 demonstrates the decrease in the temperature versus rheological power index appearing in the rheological equation. Since the variation of n through positive values results a decrease in the flow. Therefore the convective transfer of heat is compromised. This compromise of convective heat transfer leads to a decrease in temperature (see Figure 6). Moreover, the thermal region shrunk when n is increased. The parameter h_s is called the heat generation parameter and it determines the impact of the ability of the fluid to generate heat. This heat adds to the fluid to increase the temperature. Thus increasing behavior of h_s on the temperature of the fluid can be seen from Figure 7. This Figure also reflects that the hybrid nanofluid is more heat generative than the mono nanofluid. The role of thermal relaxation time on heat transfer can be seen in Figure 8. A decline in temperature against thermal relaxation time is the ability of fluid to restore its thermal equilibrium state. Therefore an increase in thermal relaxation paramater λ_E causes the thermal changes to be minimized

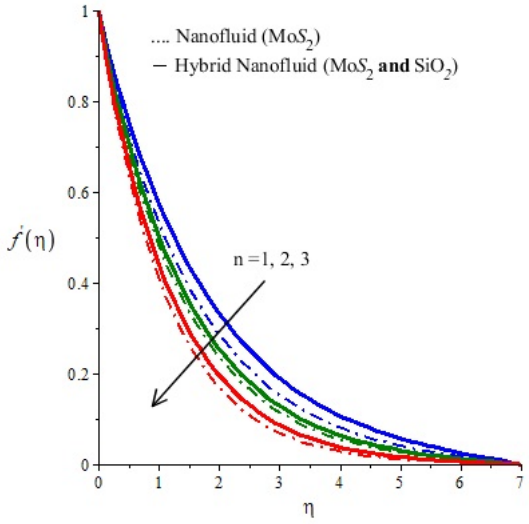

Figure 2: Horizontal velocity profiles of mono nano fluid (dotted curves) and hybrid nanofluid (solid curves) for n when $\mathrm{Pr} = 204,\ \lambda_E = 0.01,\ h_s = 1.3,\ M = 0.001,\ \varphi_1 = 0.004,\ \varphi_2 = 0.0075$.

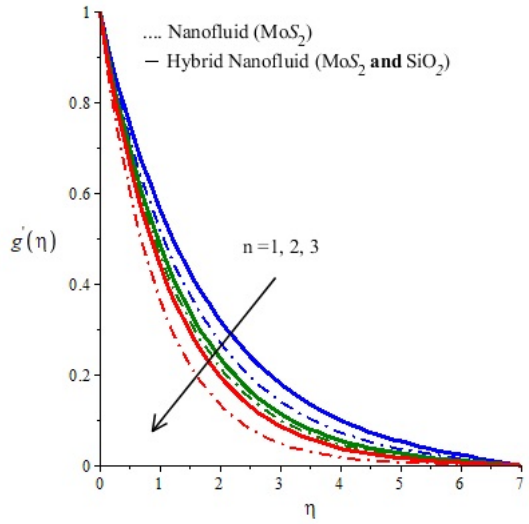

Figure 3: Vertical velocity profiles of mono nano fluid (dotted curves) and hybrid nanofluid (solid curves) for n when $\mathrm{Pr} = 204,\ \lambda_E = 0.2,\ h_s = 1.5,\ M = 0.01,\ \varphi_1 = 0.004,\ \varphi_2 = 0.0075$.

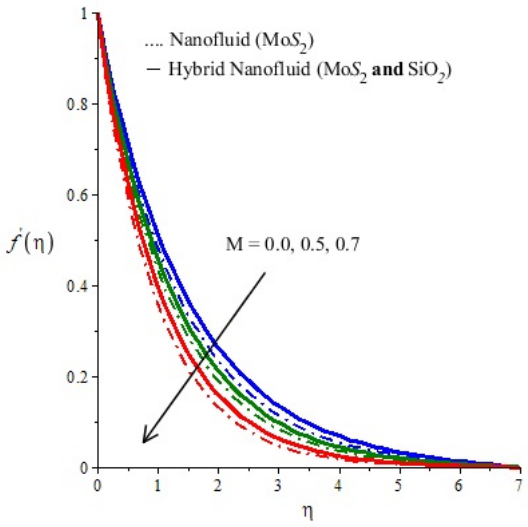

Figure 4: Horizontal velocity profiles of mono nano fluid (dotted curves) and hybrid nanofluid (solid curves) for M when $\mathrm{Pr} = 204,\ \lambda_E = 0.01,\ h_s = 1.3,\ n = 2,\ \varphi_1 = 0.004,\ \varphi_2 = 0.0075.$

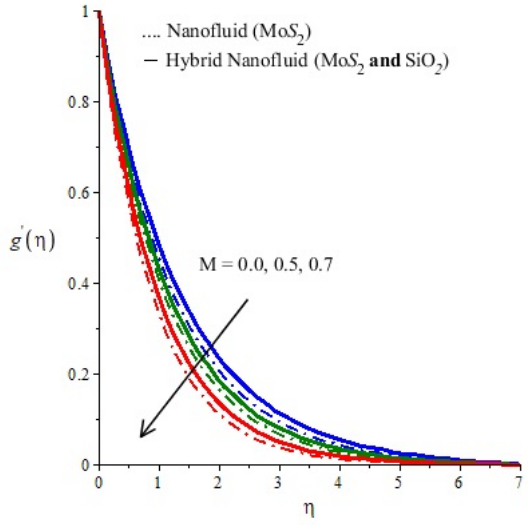

Figure 5: Vertical velocity profiles of mono nano fluid (dotted curves) and hybrid nanofluid (solid curves) for M when $\mathrm{Pr} = 204,\ \lambda_E = 0.5,\ h_s = 1.7,\ n = 2,\ \varphi_1 = 0.004,\ \varphi_2 = 0.0075.$

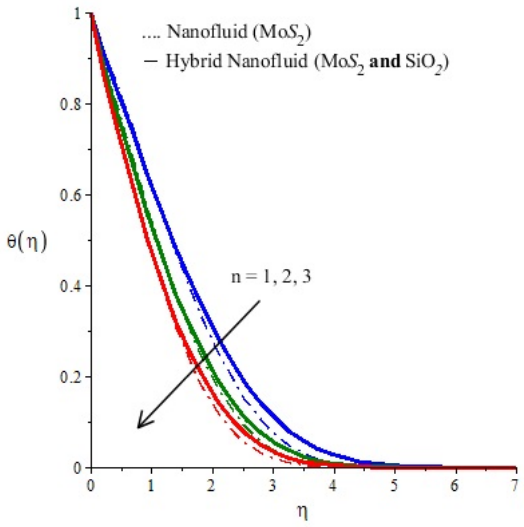

Figure 6: Temperature profiles of mono nano fluid (dotted curves) and hybrid nanofluid (solid curves) for Ec when $\Pr = 204,\ \lambda_E = 0.1,\ h_s = 1.3,\ M = 0.7,\ \varphi_1 = 0.004,\ \varphi_2 = 0.0075$.

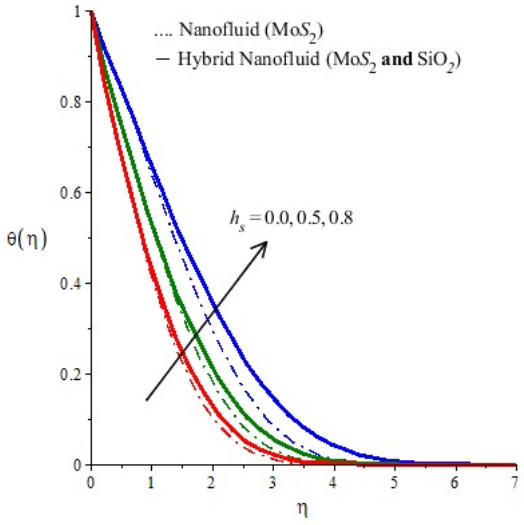

Figure 7: Temperature profiles of mono nano fluid (dotted curves) and hybrid nanofluid (solid curves) for h_s when $\Pr = 204,\ \lambda_E = 2.0,\ n = 2,\ M = 0.001,\ \varphi_1 = 0.004,\ \varphi_2 = 0.0075$.

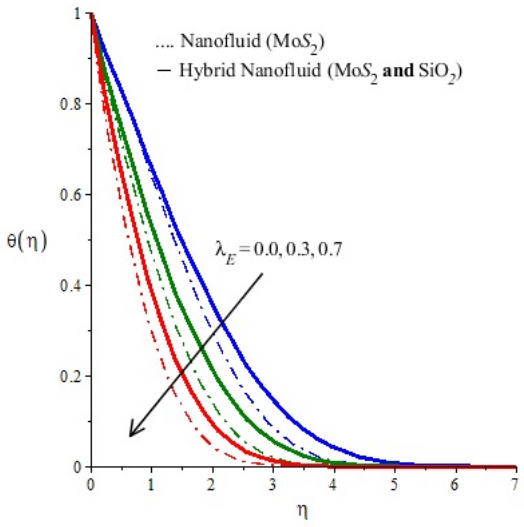

Figure 8: Temperature profiles of mono nano fluid (dotted curves) and hybrid nanofluid (solid curves) for λ_E when Pr $= 204,\ \lambda_E = 2.4,\ h_s = 1.7,\ n = 2,\ M = 0.001,\ \varphi_1 = 0.004,\ \varphi_2 = 0.0075.$

Table 3: Numerical values of velocity gradient, heat and mass fluxes versus $n,\ M,\ \lambda_E,\ K_s$ and Sc when Pr $= 204,\ \lambda_E = 0.01,\ h_s = 1.3,\ n = 2,\ M = 0.001,\ \varphi_1 = 0.004,\ \varphi_2 = 0.0075.$

		Nanofluid-MoS_2			Hybrid Nanofluid-MoS_2/SiO_2		
		$-(Re)^{-\frac{1}{2}}C_f$	$-(Re)^{-\frac{1}{2}}C_g$	$-(Re)^{-\frac{1}{2}}Nu$	$-(Re)^{-\frac{1}{2}}C_f$	$-(Re)^{-\frac{1}{2}}C_g$	$-(Re)^{-\frac{1}{2}}Nu$
n	1	0.1530038477	0.3273273303	0.07738217329	2.1904886710	2.6943502083	3.40917113
	2	0.2998837840	0.4712795494	1.878005638	2.2691491403	2.6950607774	3.408309201
	3	0.3454939329	0.4880091971	2.197857874	2.3683210301	2.7130107774	3.744985517
M	0.0	0.4445357154	0.5474239143	2.434285223	0.3921117986	0.4582307106	2.521999989
	0.3	0.5276220806	0.6161026020	2.367066226	0.2787507677	0.2383580820	2.439350498
	0.7	0.7065837651	0.7808038946	2.201385769	0.1625451271	0.1152917186	2.358610912
λ_E	0.0	0.8274144563	0.7860955489	1.489867706	0.5165267029	0.7799560991	6.085566423
	0.7	0.9577438591	0.8192032143	2.453232227	0.6269979117	0.8317641406	6.199279077
	1.3	0.9869822700	0.8511148826	2.414949813	0.6801927917	0.9024493826	5.278268369
h_s	0.0	0.4276776306	0.4728914183	3.036693234	0.3699413337	0.5672794734	8.070247557
	0.3	0.4276776306	0.4728914183	2.265464671	0.3699413337	0.5672794734	7.119296620
	0.7	0.4276776306	0.4728914183	2.189427429	0.3699413337	0.5672794734	6.162432623

Discussion about behaviors of tangential stresses and wall heat transfer rate: The behavior of tangential stresses and heat flux are examined for sampling values of n, M, λ_E and h_s for $MoS_2 - SiO_2-$ power law fluid and MoS_2- power law fluid. The parameter n appears in the rheological model designed for power law fluids. Its variation (for positive values) which are greater than 1 corresponds to the case of shear thickening whereas n has values less than 1 for shear thinning case. Shear thickening behavior of fluid makes it able to experience less wall influence and therefore, shear rate dependent viscosity decreases and as a result wall momentum penetrates into fluid slowly. Due to this fact, tangential stresses at the surface in both x and y directions become stronger. This observation is valid for both fluids ($MoS_2 - SiO_2-$ power law and MoS_2- power law). Numerical experiments have demonstrated an increase in heat transfer rate against increasing values of n greater than 1. The parameter M is called the Hartmann number and its variation determines the variation of intensity of the magnetic field. Since Lorentz force is directly proportional to the intensity of the magnetic field, therefore, flow experiences retardation due to an increase in the intensity of the magnetic field. Alternatively, one can say that an increase in M implies an increase in retardation towards flow. This increases tangential stresses in the x and $y-$ direction. Further motion due to the Lorentz force slows down and therefore, convective transport of heat is compromised. Thus convective transport of heat will be reduced and heat flux will decrease. The numerical simulations have predicted the same results (see Table 3). Thermal relaxation parameter λ_E also has a great impact on wall heat flux and therefore its behavior on heat transfer rate is examined and outcomes are displayed in Table 3. The numerical values tabulated in Table 3 show that wall heat flux for $MoS_2 - SiO_2-$ power law fluid and MoS_2- power law fluid has shown decreasing behavior versus λ_E. The heat generation parameter has also decreasing behavior on wall heat transfer rate.

5 Conclusion

Governing laws in terms of differential equations associated with a thermal enhancement in ethylene glycol due to dispersion of MoS_2 and combination of MoS_2 and SiO_2 are solved numerically by FEM. Several numerical experiments were performed. The following results are notable.

1. The comparative analysis between thermal efficiencies of MoS_2- power law fluid and

$MoS_2 - SiO_2-$ power law fluid is presented. It is found that the thermal efficiency of power law fluid with MoS_2 and SiO_2 nanostructure is greater than that of a power law with only MoS_2 nanoparticles. It is also noted that pure power law fluid has less thermal conductiv than that of MoS_2- power law fluid and $MoS_2 - SiO_2-$ power law fluid.

2. Non- Fourier heat transfer is slower than Fourier transfer due to thermal memory effects based on thermal relaxation time. Thus thermal changes are tended to be restored due to the thermal relaxation phenomenon.

3. The power law fluid with nanoparticles (MoS_2 and SiO_2) is assumed to heat generative. The numerical experiments for comparison between heat generative rate in MoS_2- power law fluid and heat generative in $MoS_2 - SiO_2-$ power law fluid are performed and it is observed that power law fluid with hybrid nanoparticles is more heat generative than power law fluid with mono- nanoparticles (MoS_2). Thus it can also be concluded that pure power law fluid is less heat generative than power law fluid with nanoparticles. Thus if power law fluid has to be used as a coolant then if it should be non- heat generative to serve as a better coolant. On the other hand power law fluid with nanoparticles serves as a stable coolant. Therefore, power law fluid serves as a better coolant if it is non-heat generative and contains hybrid nanoparticles.

4. It is found that thermal relaxation time for power law fluid with $MoS_2 - SiO_2$ nanoparticles is lesser than that for power law fluid with MoS_2 nanoparticles. Thus power law fluid with MoS_2 and SiO_2 is more capable to restore thermal changes than that of power law fluid with MoS_2 nanoparticles only.

5. Magnetic field is responsible for inducing Lorentz force which is responsible for creating shear stresses on the surface. Thus tangential stresses are increased by increasing the magnetic field intensity.

6. Heat flux decreases when the heat generative parameter is increased.

7. There is a significant difference between heat fluxes for MoS_2 power law fluid and $MoS_2 - SiO_2-$ power law fluid. Thus the use of $MoS_2 - SiO_2-$ power law fluid is recommended as it has much greater heat flux than that of MoS_2- power law fluid.

Acknowledgment: The author wishes to express his thanks for the financial support received under Project ID SB201020 from King Fahd University of Petroleum and Minerals.

Conflict of interest: I wish to confirm that there are no known conflicts of interest associated with this publication and there is financial support for this work that is acknowledged.

Author declaration: I declare the adherence of ethics and rules by journal and publishing company

References

[1] Srinivasacharya, D., & Reddy, G. S. Chemical reaction and radiation effects on mixed convection heat and mass transfer over a vertical plate in power-law fluid saturated porous medium. Journal of the Egyptian Mathematical Society, 24(1), 108-115, (2016).

[2] Machireddy, G. R., & Naramgari, S. Heat and mass transfer in radiative MHD Carreau fluid with cross diffusion. Ain Shams Engineering Journal, 9(4), 1189-1204 (2018).

[3] Hayat, T., Farooq, S., Alsaedi, A., & Ahmad, B. Hall and radial magnetic field effects on radiative peristaltic flow of Carreau–Yasuda fluid in a channel with convective heat and mass transfer. Journal of Magnetism and Magnetic Materials, 412, 207-216, (2016).

[4] Akram, S., Nadeem, S., & Hussain, A. Effects of heat and mass transfer on peristaltic flow of a Bingham fluid in the presence of inclined magnetic field and channel with different wave forms. Journal of Magnetism and Magnetic Materials, 362, 184-192, (2014).

[5] Raju, C. S. K., Sandeep, N., Sugunamma, V., Babu, M. J., & Reddy, J. R. Heat and mass transfer in magnetohydrodynamic Casson fluid over an exponentially permeable stretching surface. Engineering Science and Technology, an International Journal, 19(1), 45-52, (2016).

[6] Nadeem, S., & Akbar, N. S. Influence of heat transfer on a peristaltic transport of Herschel–Bulkley fluid in a non-uniform inclined tube. Communications in Nonlinear Science and Numerical Simulation, 14(12), 4100-4113, (2009).

[7] Minakov A V, Rudyak A Ya, Pryazhnikov M.I, Rheological behavior of water and ethylene glycol based nanofluids containing oxide nanoparticles, Colloids and Sur-

faces A: Physicochemical and Engineering Aspects. 5 October; 554: 279-285, 2018. https://doi.org/10.1016/j.colsurfa.2018.06.051

[8] Nawaz, M., Nazir, U., Alharbi, S. O., & Elmasry, Y. Compuational study on transport of thermal energy and mass species in power law rheological fluid with hybrid nanostructures in the presence of chemical reaction. International Communications in Heat and Mass Transfer, 120, 105022, (2021).

[9] Cheng, C. Y. Combined heat and mass transfer in natural convection flow from a vertical wavy surface in a power-law fluid saturated porous medium with thermal and mass stratification. International Communications in Heat and Mass Transfer, 36(4), 351-356, (2009).

[10] Khan, W. A., & Reddy Gorla, R. S. Heat and mass transfer in power-law nanofluids over a nonisothermal stretching wall with convective boundary condition. Journal of heat transfer, 134(11), (2012).

[11] Sarafan, M. J., Alizadeh, R., Fattahi, A., Ardalan, M. V., & Karimi, N. Heat and mass transfer and thermodynamic analysis of power-law fluid flow in a porous microchannel. Journal of Thermal Analysis and Calorimetry, 141(5), 2145-2164, (2020).

[12] Pal, D., & Chatterjee, S. Soret and Dufour effects on MHD convective heat and mass transfer of a power-law fluid over an inclined plate with variable thermal conductivity in a porous medium. Applied Mathematics and Computation, 219(14), 7556-7574, (2013).

[13] El-Kabeir, S. M. M., Chamkha, A., & Rashad, A. M. Heat and mass transfer by MHD stagnation-point flow of a power-law fluid towards a stretching surface with radiation, chemical reaction and Soret and Dufour effects. International journal of chemical reactor engineering, 8(1), (2010).

[14] Dogonchi, A. S., & Ganji, D. D. Thermal radiation effect on the nano-fluid buoyancy flow and heat transfer over a stretching sheet considering Brownian motion. Journal of Molecular Liquids, 223, 521-527,(2016).

[15] Dogonchi, A. S., Chamkha, A. J., Seyyedi, S. M., Hashemi-Tilehnoee, M., & Ganji, D. D. Viscous dissipation impact on free convection flow of Cu-water nanofluid in a

circular enclosure with porosity considering internal heat source. Journal of Applied and Computational Mechanics, 5(4), 717-726, (2019).

[16] Sheikholeslami, M., Abelman, S., & Ganji, D. D. Numerical simulation of MHD nanofluid flow and heat transfer considering viscous dissipation. International Journal of Heat and Mass Transfer, 79, 212-222, (2014).

[17] Sheikholeslami, M., & Sadoughi, M. Mesoscopic method for MHD nanofluid flow inside a porous cavity considering various shapes of nanoparticles. International Journal of Heat and Mass Transfer, 113, 106-114, (2017).

[18] Qureshi, I. H., Nawaz, M., Abdel-Sattar, M. A., Aly, S., & Awais, M. Numerical study of heat and mass transfer in MHD flow of nanofluid in a porous medium with Soret and Dufour effects. Heat Transfer, (2021).

[19] Nawaz, M., Hayat, T., & Alsaedi, A. Dufour and Soret effects on MHD flow of viscous fluid between radially stretching sheets in porous medium. Applied Mathematics and Mechanics, 33(11), 1403-1418, (2012).

[20] Hayat, T., Sajjad, R., Ellahi, R., Alsaedi, A., & Muhammad, T. Homogeneous-heterogeneous reactions in MHD flow of micropolar fluid by a curved stretching surface. Journal of Molecular Liquids, 240, 209-220, (2017).

[21] Nawaz, M., Saleem, S., & Rana, S. Computational study of chemical reactions during heat and mass transfer in magnetized partially ionized nanofluid. Journal of the Brazilian Society of Mechanical Sciences and Engineering, 41(8), 1-15, (2019).

[22] Qureshi, I. H., Nawaz, M., Abdel-Sattar, M. A., Aly, S., & Awais, M. Numerical study of heat and mass transfer in MHD flow of nanofluid in a porous medium with Soret and Dufour effects. Heat Transfer, (2021).

[23] Ellahi, R., Zeeshan, A., Hussain, F., & Asadollahi, A. Peristaltic blood flow of couple stress fluid suspended with nanoparticles under the influence of chemical reaction and activation energy. Symmetry, 11(2), 276, (2019).

[24] Sheikholeslami, M., Zeeshan, A., & Majeed, A. Control volume based finite element simulation of magnetic nanofluid flow and heat transport in non-Darcy medium. Journal of Molecular Liquids, 268, 354-364, (2018).

[25] Sandeep, N., & Kumar, M. S. Heat and Mass Transfer in Nanofluid Flow over an Inclined Stretching Sheet with Volume Fraction of Dust and Nanoparticles. Journal of Applied Fluid Mechanics, 9(5), (2016).

[26] Qi, C., Liang, L., & Rao, Z. Study on the flow and heat transfer of liquid metal based nanofluid with different nanoparticle radiuses using two-phase lattice Boltzmann method. International Journal of Heat and Mass Transfer, 94, 316-326, (2016).

[27] Gheynani, A. R., Akbari, O. A., Zarringhalam, M., Shabani, G. A. S., Alnaqi, A. A., Goodarzi, M., & Toghraie, D. Investigating the effect of nanoparticles diameter on turbulent flow and heat transfer properties of non-Newtonian carboxymethyl cellulose/CuO fluid in a microtube. International Journal of Numerical Methods for Heat & Fluid Flow, (2019).

[28] Ahmad, S., Ali, K., Rizwan, M., & Ashraf, M. Heat and mass transfer attributes of copper–aluminum oxide hybrid nanoparticles flow through a porous medium. Case Studies in Thermal Engineering, 25, 100932, (2021).

[29] Ghadikolaei, S. S., Hosseinzadeh, K., & Ganji, D. D. Investigation on ethylene glycol-water mixture fluid suspend by hybrid nanoparticles (TiO2-CuO) over rotating cone with considering nanoparticles shape factor. Journal of Molecular Liquids, 272, 226-236, (2018).

[30] Alharbi, S. O. Impact of hybrid nanoparticles on transport mechanism in magneto-hydrodynamic fluid flow exposed to induced magnetic field. Ain Shams Engineering Journal, 12(1), 995-1000, (2021).

[31] Ramesh, G. K., Roopa, G. S., Shehzad, S., & Khan, S. U. Interaction of Al2O3-Ag and Al2O3-Cu hybrid nanoparticles with water on convectively heated moving material. Multidiscipline Modeling in Materials and Structures, (2020).

[32] Hosseinzadeh, K., Asadi, A., Mogharrebi, A. R., Azari, M. E., & Ganji, D. D. (2021). Investigation of mixture fluid suspended by hybrid nanoparticles over vertical cylinder by considering shape factor effect. Journal of Thermal Analysis and Calorimetry, 143(2), 1081-1095.

[33] Sreedevi, P., Reddy, P. S., & Chamkha, A. Heat and mass transfer analysis of unsteady hybrid nanofluid flow over a stretching sheet with thermal radiation. SN Applied Sciences, 2(7), 1-15, (2020).

[34] Alharbi, S. O., Nawaz, M., & Nazir, U. Thermal analysis for hybrid nanofluid past a cylinder exposed to magnetic field. AIP Advances, 9(11), 115022, (2019).

[35] Copelli, S., Torretta, V., Pasturenzi, C., Derudi, M., Cattaneo, C. S., & Rota, R. On the divergence criterion for runaway detection: Application to complex controlled systems. Journal of loss prevention in the process industries, 28, 92-100, (2014).

[36] Christov, C. I. On frame indifferent formulation of the Maxwell–Cattaneo model of finite-speed heat conduction. Mechanics Research Communications, 36(4), 481-486, (2009).

[37] Sui, J., Zheng, L., & Zhang, X. Boundary layer heat and mass transfer with Cattaneo–Christov double-diffusion in upper-convected Maxwell nanofluid past a stretching sheet with slip velocity. International Journal of Thermal Sciences, 104, 461-468, (2016).

[38] Hafeez, A., Khan, M., & Ahmed, J. Flow of Oldroyd-B fluid over a rotating disk with Cattaneo–Christov theory for heat and mass fluxes. Computer methods and programs in biomedicine, 191, 105374, (2020).

[39] Makinde, O. D., Sandeep, N., Animasaun, I. L., & Tshehla, M. S. Numerical exploration of Cattaneo-Christov heat flux and mass transfer in magnetohydrodynamic flow over various geometries. In Defect and Diffusion Forum (Vol. 374, pp. 67-82). Trans Tech Publications Ltd, (2017).

[40] Bai, Y., Xie, B., Zhang, Y., Cao, Y., & Shen, Y. Stagnation-point flow and heat transfer of upper-convected Oldroyd-B MHD nanofluid with Cattaneo–Christov double-diffusion model. International Journal of Numerical Methods for Heat & Fluid Flow, (2019).

[41] Hayat, T., Aziz, A., Muhammad, T., & Alsaedi, A. Three-dimensional flow of Prandtl fluid with Cattaneo-Christov double diffusion. Results in Physics, 9, 290-296, (2018).

[42] Khan, W. A., Khan, M., & Alshomrani, A. S. Impact of chemical processes on 3D Burgers fluid utilizing Cattaneo-Christov double-diffusion: applications of non-Fourier's

heat and non-Fick's mass flux models. Journal of Molecular Liquids, 223, 1039-1047, (2016).

[43] Zhuang, Y. J., Yu, H. Z., & Zhu, Q. Y. A thermal non-equilibrium model for 3D double diffusive convection of power-law fluids with chemical reaction in the porous medium. International Journal of Heat and Mass Transfer, 115, 670-694, (2017).